

## Supporting Information

### **Enhanced photodetection and a wider spectral range in In<sub>2</sub>S<sub>3</sub>-ZnO 2D-3D heterojunction: Combined optical absorption and enhanced carrier separation at the type-II heterojunction**

**Narinder Kaur<sup>1</sup>, Abhishek Ghosh<sup>1</sup>, Prashant Bisht<sup>1</sup>, Arvind Kumar<sup>1</sup>, Vishakha Kaushik<sup>1</sup>, Nisha Kodan<sup>1</sup>, Rajendra Singh<sup>1</sup>, and B.R. Mehta<sup>1,2\*</sup>**

*1 Thin Film Laboratory, Department of Physics, Indian Institute of Technology Delhi, New Delhi, 110016, India)*

*2 Directorate of Research, Innovation, and Development, Jaypee Institute of Information technology, Noida (U.P.), 201309, India*

*Author to whom correspondence to be addressed\* **Email: [brmehta@physics.iitd.ac.in](mailto:brmehta@physics.iitd.ac.in)***

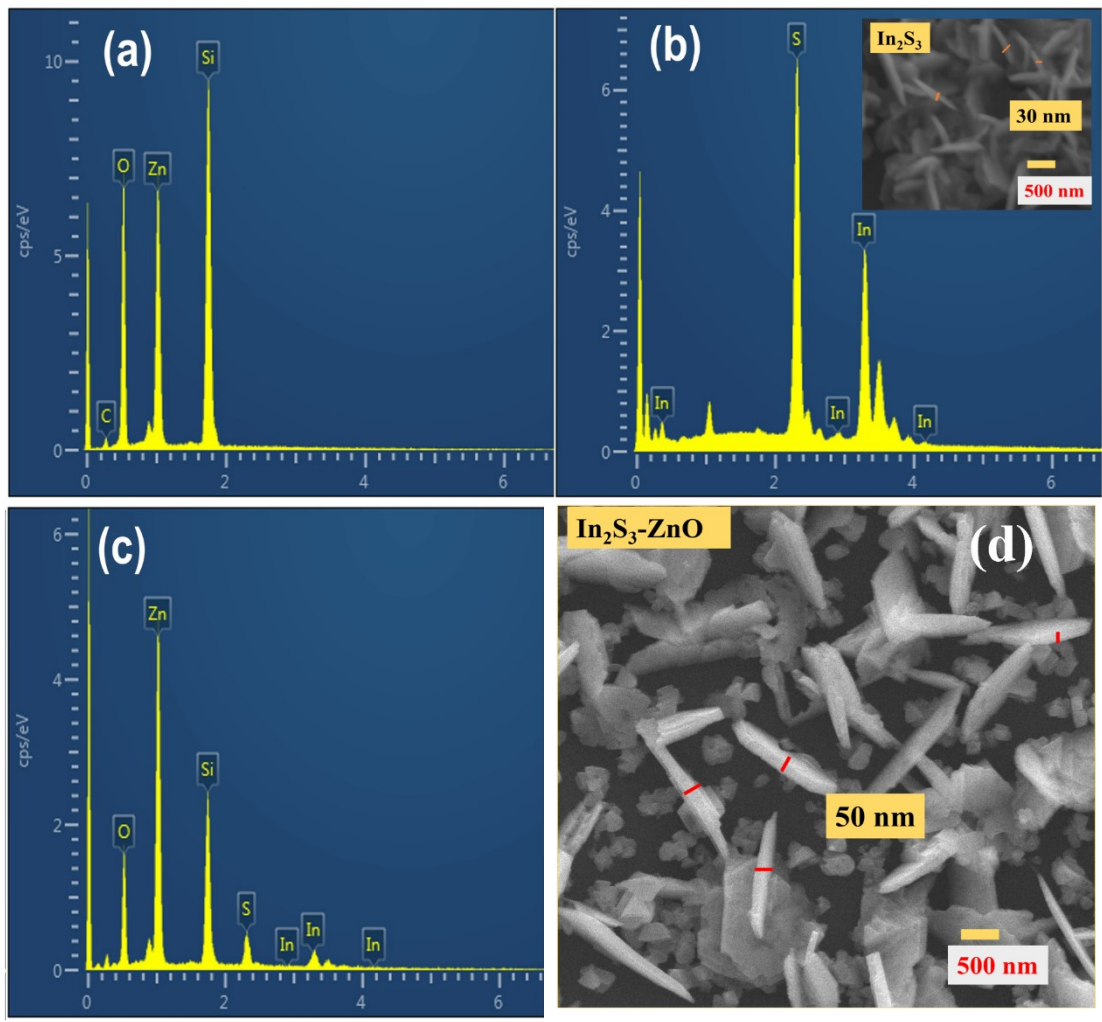


Figure S1 (a) EDX for ZnO, (b) EDX for  $\text{In}_2\text{S}_3$  with cross-sectional image of  $\text{In}_2\text{S}_3$  in the inset, (c) EDX for the  $\text{In}_2\text{S}_3/\text{ZnO}$  heterojunction (d) cross-sectional image of the heterojunction showing

The chemical composition of the samples is analyzed by EDX spectra which show the presence of Zn and O in the ZnO thin films with In and S elements present non continuously in the 2D- $\text{In}_2\text{S}_3$  and continuous presence of Zn, O, In, and S in the  $\text{In}_2\text{S}_3\text{-ZnO}$  heterojunction sample.



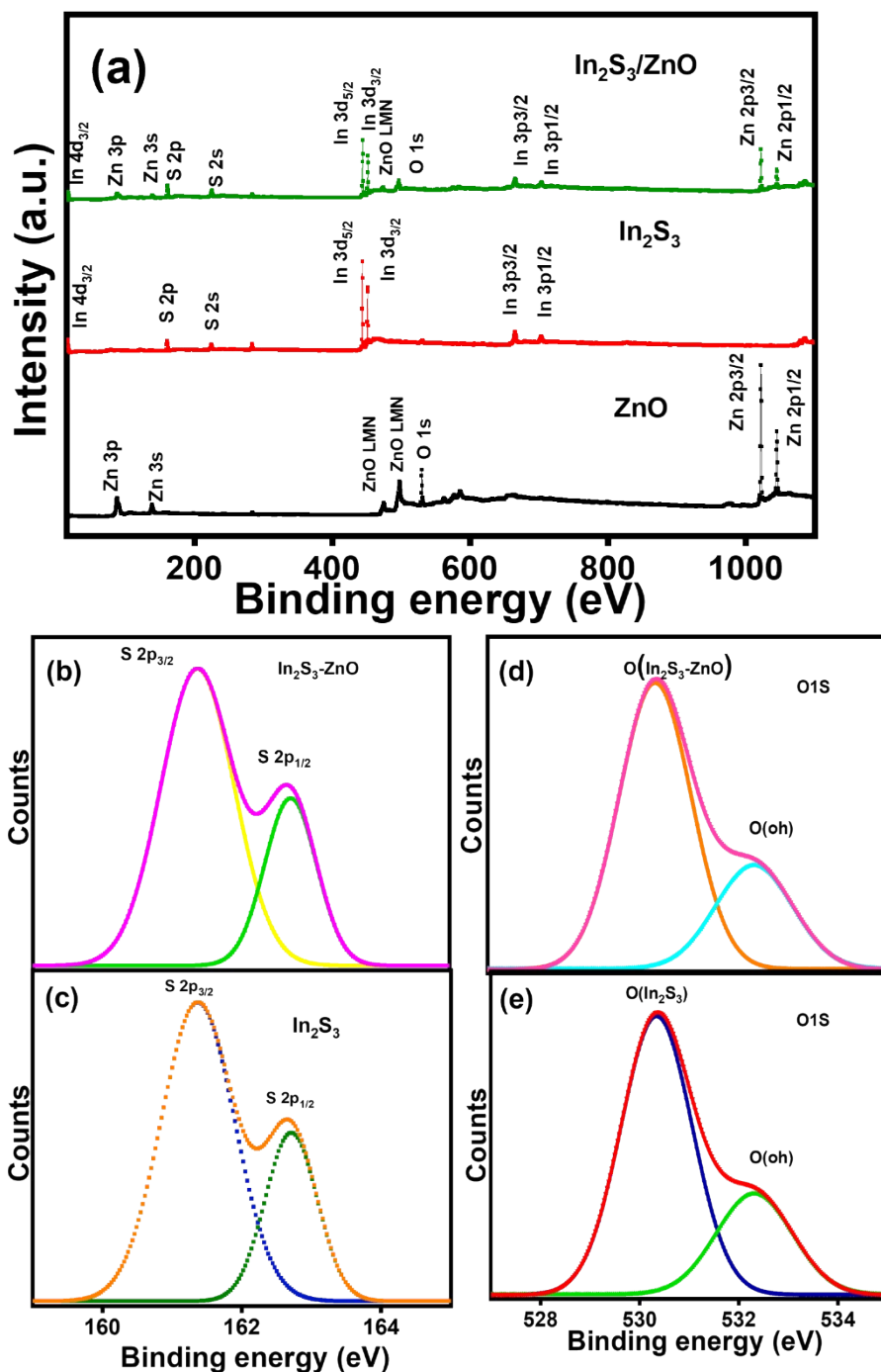
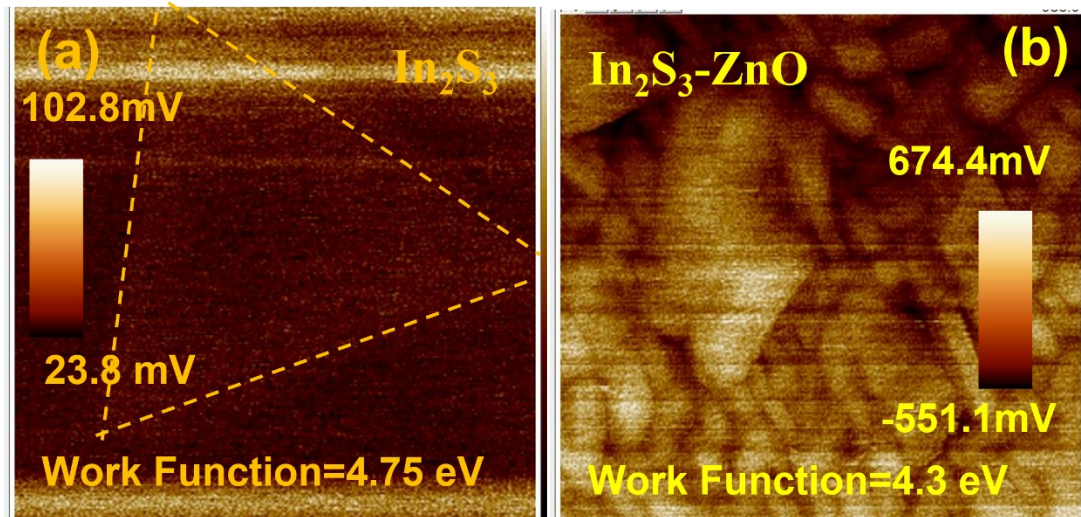


Figure S2(a) Survey spectra for the pristine  $\text{In}_2\text{S}_3$ ,  $\text{ZnO}$  and  $\text{In}_2\text{S}_3$ - $\text{ZnO}$  heterojunction sample, show the presence of In, S, Zn and O over the entire sample, these results are consistent with EDX spectra. (b) and (c) the deconvoluted spectra for sulfur present in both pristine  $\text{In}_2\text{S}_3$  and the  $\text{In}_2\text{S}_3$ - $\text{ZnO}$  heterojunction (d) and (e) the deconvoluted spectra for oxygen in both  $\text{ZnO}$  and the heterojunction  $\text{In}_2\text{S}_3$ - $\text{ZnO}$ .

Figure S3 (a) and (b) have shown AFM potential images for the  $\text{In}_2\text{S}_3$  and the  $\text{In}_2\text{S}_3\text{-ZnO}$  heterojunction with the thickness of nanoflakes around 30 nm for pristine  $\text{In}_2\text{S}_3$  and 50 nm for the  $\text{In}_2\text{S}_3\text{-ZnO}$  heterojunction. The work function value is 4.75 eV for the  $\text{In}_2\text{S}_3$  and 4.3 eV



for the heterojunction which implies that both behave differently in the photoresponse.

For pristine ZnO, photocurrent values are of the order of  $7 \times 10^{-7}$  A and dark current  $3.9 \times 10^{-7}$  A. For  $\text{In}_2\text{S}_3$ , the current is the order of  $4 \times 10^{-5}$  A and dark current  $1.4 \times 10^{-5}$  A at +1 V, while in the  $\text{In}_2\text{S}_3\text{-ZnO}$  heterojunction sample, the current in light is of the order of  $0.28 \times 10^{-3}$  A which is  $10^4$  and  $10^2$  times higher than pristine ZnO and  $\text{In}_2\text{S}_3$  respectively.

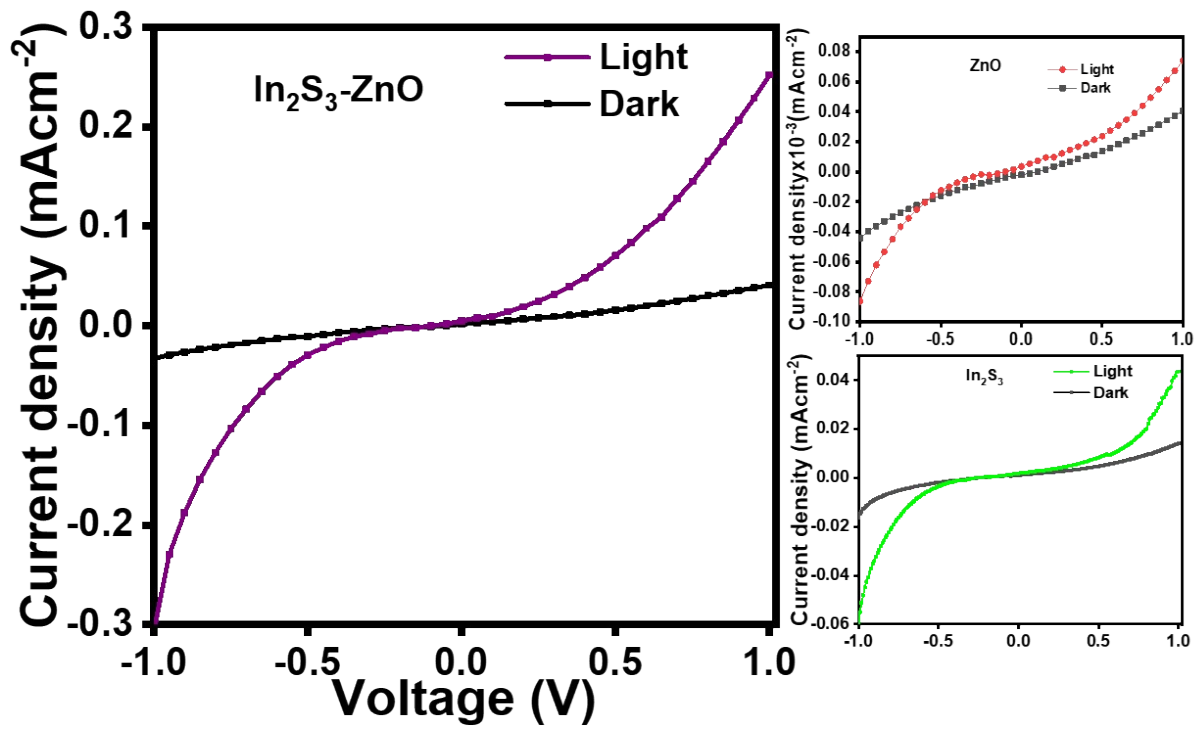


Figure S4 shows I-V characteristics (current density variation with voltage) under dark and white light illumination for  $\text{In}_2\text{S}_3\text{-ZnO}$  heterojunction, pristine  $\text{In}_2\text{S}_3$ , and  $\text{ZnO}$  thin film samples.

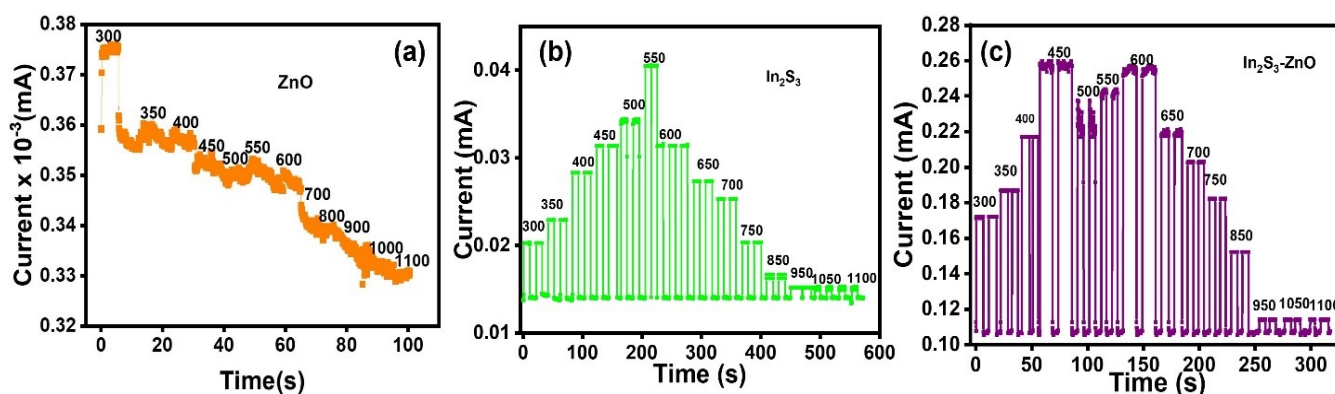


Figure S5 (a) ZnO thin films of the thickness of 100 nm exhibit a high response of  $3.2 \times 10^{-4}$  mAcm<sup>-2</sup> at wavelength 300 nm in the UV region and a minimal  $2.5 \times 10^{-5}$  mAcm<sup>-2</sup> response for the visible wavelength range 400-700 nm, because of its wide bandgap (3.2 eV) value. (b) Nanoflakes of In<sub>2</sub>S<sub>3</sub> show photoresponse in the visible region of 400-800 nm, which includes a maximum current of 0.05 mAcm<sup>-2</sup> for the 550 nm wavelength close to the bandgap (2.2 eV) of In<sub>2</sub>S<sub>3</sub> and a current of 0.02 mAcm<sup>-2</sup> for wavelength 800 nm. (c) In<sub>2</sub>S<sub>3</sub>-ZnO heterojunction exhibits higher photoresponse and current density within the entire UV-Visible wavelength range of 300-800 nm with a maximum photocurrent value of 0.3 mAcm<sup>-2</sup> at the wavelength 450 nm. The measurements also revealed that the heterojunction shows more photocurrent than the ZnO and In<sub>2</sub>S<sub>3</sub> samples for the entire UV-Vis range.

## References

1. Yu Zhao, Daizhe Yu, Jianting Lu, Li Tao, Zefeng Chen, Yibin Yang, Aixiang Wei, Lili Tao, Jun Liu, Zhaoqiang Zheng, Mingming Hao, and Jian-Bin Xu, "Thickness-Dependent Optical Properties and In-Plane Anisotropic Raman Response of the 2D  $\beta$ -In<sub>2</sub>S<sub>3</sub>, Adv.Optical Mater. 2019, 7, 1901085.

2. Narinder Kaur, Dipika Sharma, B.R. Mehta, “Growth of In<sub>2</sub>S<sub>3</sub> nanolayers on F-Mica, SiO<sub>2</sub>, ZnO, and TiO<sub>2</sub> substrates using chemical vapor deposition” *Materials Science & Engineering B* 264 (2021) 114889.
3. Di Wu, Yuange Wang, Longhui Zeng, Cheng Jia, Enping Wu, Tingting Xu, Zhifeng Shi, Yongtao Tian, Xinjian Li, and Yuen Hong Tsang, “Design of 2D Layered PtSe<sub>2</sub> Heterojunction for the High-Performance, Room-Temperature, Broadband, Infrared Photodetector”, *ACS Photonics* **2018** 5 (9), 3820-3827 DOI: 10.1021/acsp Photonics.8b00853.
4. Jongtae Ahn, Ji-Hoon Kyhm, Hee Kyoung Kang, Namhee Kwon, Hong-Kyu Kim, Soohyung Park, and Do Kyung Hwang, “2D MoTe<sub>2</sub>/ReS<sub>2</sub> van der Waals Heterostructure for High-Performance and Linear Polarization-Sensitive Photodetector”, *ACS Photonics* 2021 8 (9), 2650-2658 DOI: 10.1021/acsp Photonics.1c00598.
5. Xinglin Wen, Sijie Chen, Jiabin Zhao, Wei Du, and Weijie Zhao, “Enhanced Plasmonic Hot-Carrier Transfer in Au/WS<sub>2</sub> Heterojunctions under Nonequilibrium Condition”, *ACS Photonics* Article ASAP DOI: 10.1021/acsp Photonics.1c01938.